Appendix of Noise Aware Scheduling in Data Centers

Hameedah Sultan
School of Information Technology
Indian Institute of Technology
New Delhi, 110016
hameedah.sultan@gmail.com

Arpit Katiyar
Samsung Research Lab
Noida, Uttar Pradesh 201303
akatiyar.cse.iitd@gmail.com

Smruti R. Sarangi
Computer Science and Engg.
Indian Institute of Technology
New Delhi, 110016
srsarangi@cse.iitd.ac.in

A. SOUND PROPAGATION IN A MEDIUM

A sound wave traveling in air causes oscillations in pressure above or below the ambient atmospheric pressure. In acoustic theory, a sound source is mainly characterized by its amplitude and frequency (f). The acoustic incident pressure field ($\widetilde{p}$) at an observation point, x, due to a point source located at x_s is given by Equation 1 where, $\omega = 2\pi f$, c_0 is the speed of sound and $\widetilde{S}$ represents the source amplitude.

$$\widetilde{p}\,(x,\omega) = \widetilde{S}\,\frac{e^{-j\omega|x-x_s|/c_0}}{4\pi \mid x - x_s \mid} \tag{1}$$

The relationship between power (P in Watts), and the amplitude, $\widetilde{S}$, is:

$$P = \frac{2\pi \mid \widetilde{S} \mid^2}{c_0\rho} \tag{2}$$

where, ρ is the density of air.

The pressure field calculated using Equation 1 is valid for an acoustic source present in an open space without absorption of sound. In a realistic situation with boundaries we have reflection, transmittance, scattering, and absorption. Hence, in such realistic situations, the final acoustic field is calculated by taking into consideration all of these factors. Given absorption and reflection coefficients[1] of the boundary surface, the amplitude of these waves can be calculated using radiation transport theory. The field induced by Equation 1 when we have absorption is the solution of the non-homogeneous Helmholtz equation:

$$\nabla^2\widetilde{p} + \kappa^2\widetilde{p} = 4\pi\widetilde{S}\delta\,(x - x_s) \tag{3}$$

where, $\kappa = s/c_0$ is the complex wave number, with $s = j\omega$ being the Laplace variable.

When the acoustic wave is incident upon a boundary, the incident field ($\widetilde{p}$) and its normal derivative satisfy:

$$\begin{aligned}\gamma\,(x,\kappa)\,\widetilde{p}\,(x,\kappa) + \lambda\,(x,\kappa)\,\frac{\partial\widetilde{p}\,(x,\kappa)}{\partial n} \\ = \widetilde{f}\,(x,\kappa) + \widetilde{g}\,(\kappa)\cdot\mathbf{n}\,(x)\,, \quad for\, x \in \partial V\end{aligned} \tag{4}$$

[1]The sound absorption coefficient or surface absorptivity (α) indicates the amount of acoustic energy absorbed by a surface when an acoustic wave is incident upon it. It is the ratio of the absorbed intensity to the incident intensity. Similarly, the reflection coefficient is the ratio of the reflected intensity to the incident intensity.

Here, $\mathbf{n}\,(x)$ is the normal vector at point x, while γ, λ and $\widetilde{f}$ are known complex functions of position and frequency, and $\widetilde{g}$ is independent of position. The above equation is used to calculate the total field at a boundary point and also the impact of the boundary surface on other points. Specifying a boundary condition is simply initializing γ, λ, and vectors $\widetilde{f}$, $\widetilde{\mathbf{g}}$ with appropriate values. When the acoustic wave is incident on a locally impedant wall, the boundary condition is given by:

$$\frac{\partial\widetilde{p}}{\partial n} - \frac{\rho s}{Z}\widetilde{p} = 0 \tag{5}$$

where, Z is the acoustic impedance of the medium. $Z(\omega)$ indicates the amount of sound pressure generated by the vibration of its molecules at a given frequency (f). For a given boundary surface, we can calculate Z and γ using Equations 6 and 7, respectively.

$$Z = Re\,(Z(\omega)) = \rho c_0\alpha\,(\omega) \tag{6}$$

where, ρ is the density of air and $\alpha\,(\omega)$ is the surface absorptivity for a given ω.

$$\gamma = -j\frac{\omega\rho}{Z} \tag{7}$$

B. SPL PROFILE OF THE DATA CENTER

Figures 1–12 show the SPL distribution for different cases of scenario I.

In all the three scenarios and for all the cases, the maximum temperature during simulation never exceeds the threshold temperature. In Appendix C, Figures 23 to 31 show the temperature profile inside the data center for uniform workload distribution, heuristic-I and heuristic-II for scenario-I. For other scenarios also the maximum temperature inside the data center is around 30 °C.

For heuristic-II, the SPL profiles obtained are shown in Figures 13-22 for various locations of interest.

C. THERMAL PROFILE OF THE DATA CENTER

The temperature diagrams below (Figures 23 to 30) show how the thermal profile inside the data center changes for scenario-I as we consider various locations for noise reduction.

D. POWER CONSUMPTION OF DIFFERENT BENCHMARKS

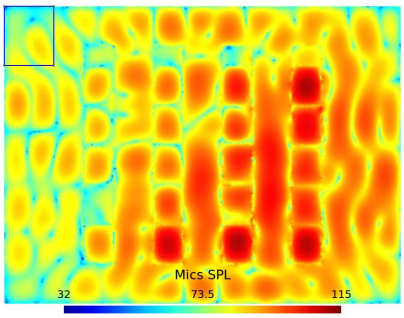

Figure 3: SPL distribution on microphones plane after workload redistribution for corner office with heuristic-I for scenario-I

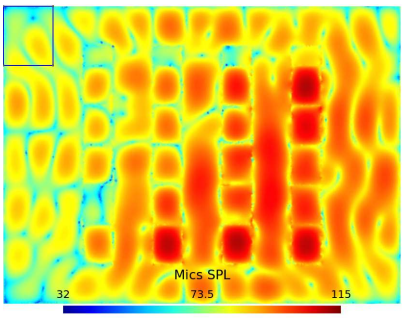

Figure 4: SPL distribution on microphones plane after workload redistribution for corner office with heuristic-II for scenario-I

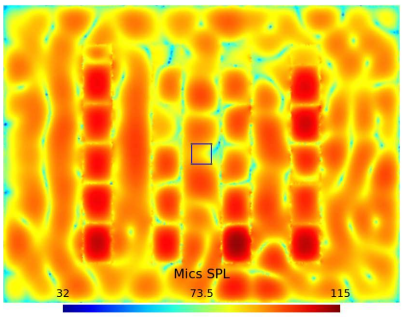

Figure 5: SPL distribution on microphones plane after workload redistribution for mobile worker with heuristic-I for scenario-I

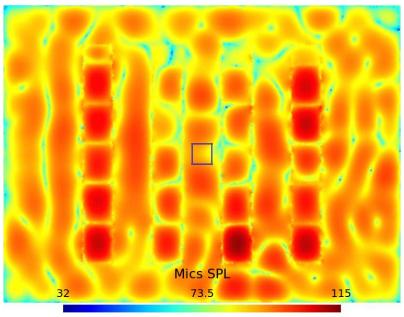

Figure 6: SPL distribution on microphones plane after workload redistribution for mobile worker with heuristic-II for scenario-I

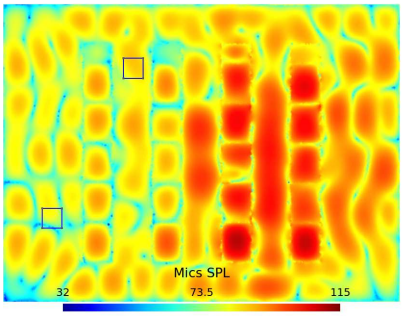

Figure 7: SPL distribution on microphones plane after workload redistribution for multiple workers with heuristic-I for scenario-I

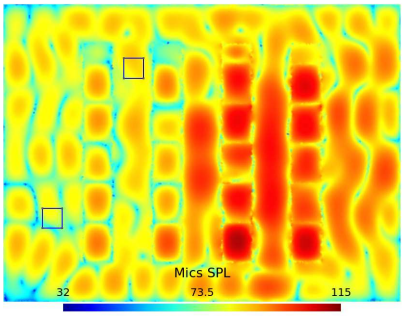

Figure 8: SPL distribution on microphones plane after workload redistribution for multiple workers with heuristic-II for scenario-I

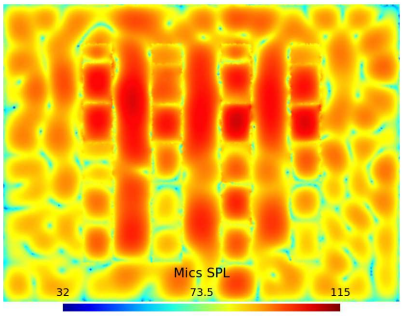

Figure 9: SPL distribution on microphones plane after workload redistribution for side wall with heuristic-I for scenario-I

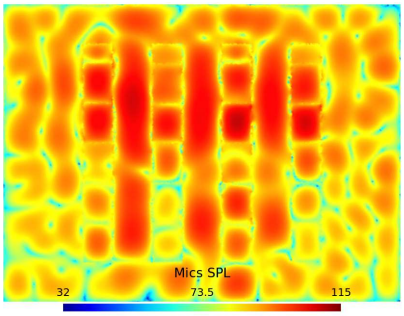

Figure 10: SPL distribution on microphones plane after workload redistribution for side wall with heuristic-II for scenario-I

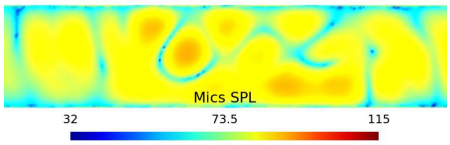

Figure 11: SPL distribution on the data center wall for heuristic-I for scenario-I

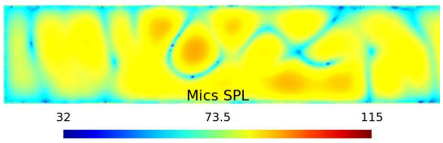

Figure 12: SPL distribution on the data center wall for heuristic-II for scenario-I

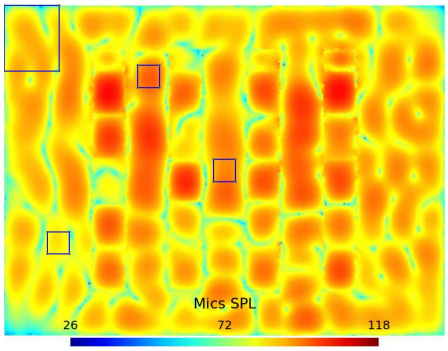

Figure 13: SPL distribution on microphones plane for uniform workload distribution for scenario-II

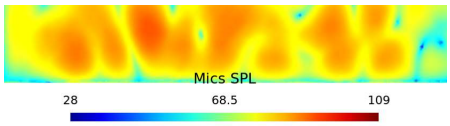

Figure 14: SPL distribution on the data center wall for uniform distribution for scenario-II

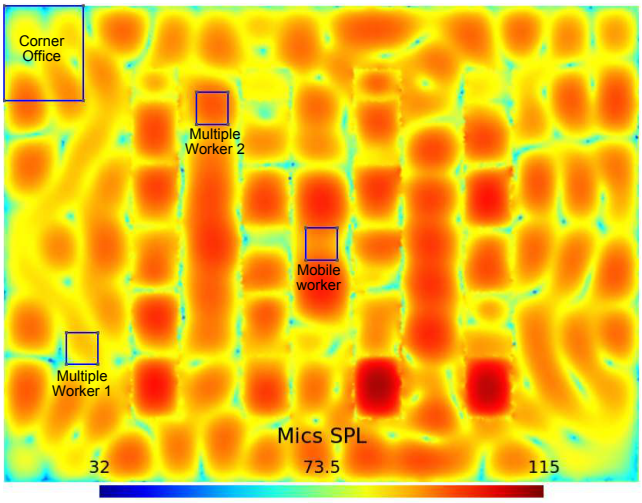

Figure 1: SPL distribution on microphones plane for uniform workload distribution for scenario-I

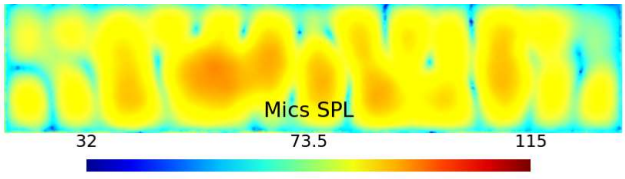

Figure 2: SPL distribution on the data center wall for uniform distribution for scenario-I

Table 1 shows the power consumed by different benchmarks measured using a loop ammeter.

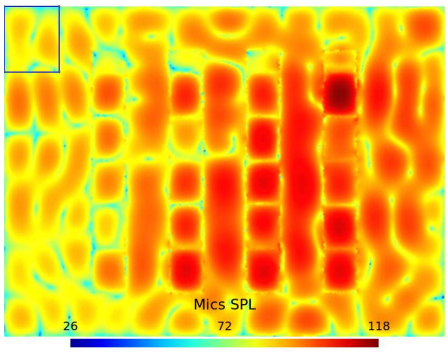

Figure 15: SPL distribution on microphones plane after workload redistribution for corner office with heuristic-I for scenario-II

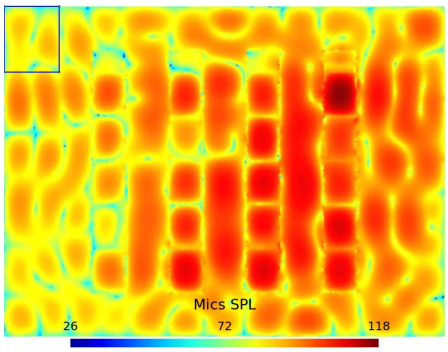

Figure 16: SPL distribution on microphones plane after workload redistribution for corner office with heuristic-II for scenario-II

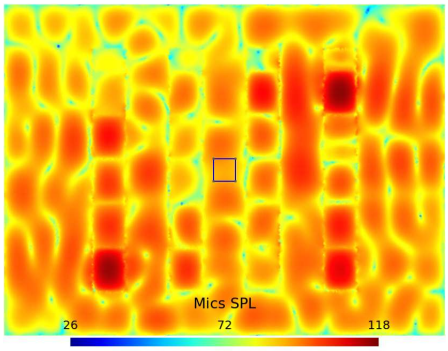

Figure 17: SPL distribution on microphones plane after workload redistribution for mobile worker with heuristic-I for scenario-II

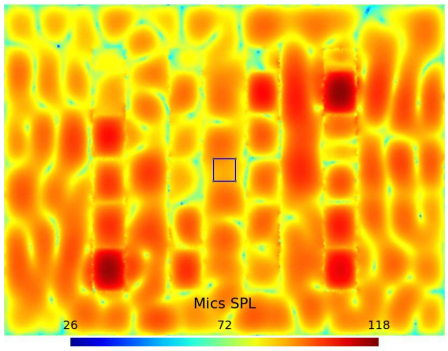

Figure 18: SPL distribution on microphones plane after workload redistribution for mobile worker with heuristic-II for scenario-II

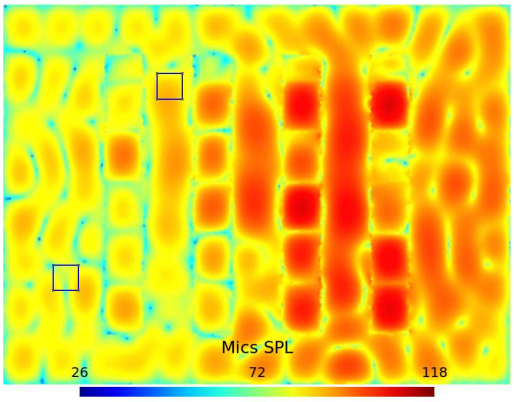

Figure 19: SPL distribution on microphones plane after workload redistribution for multiple workers with heuristic-I for scenario-II

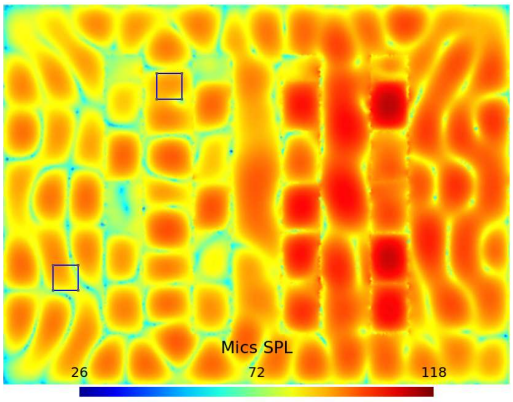

Figure 20: SPL distribution on microphones plane after workload redistribution for multiple workers with heuristic-II for scenario-II

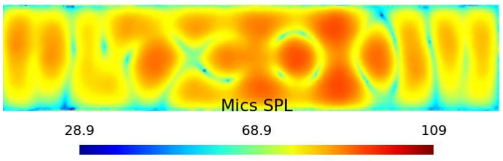

Figure 21: SPL distribution on the data center wall with heuristic-I for scenario-II

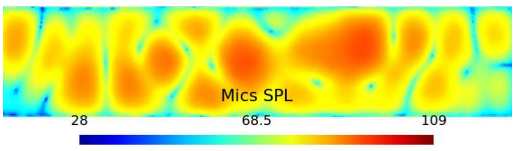

Figure 22: SPL distribution on the data center wall with heuristic-II for scenario-II

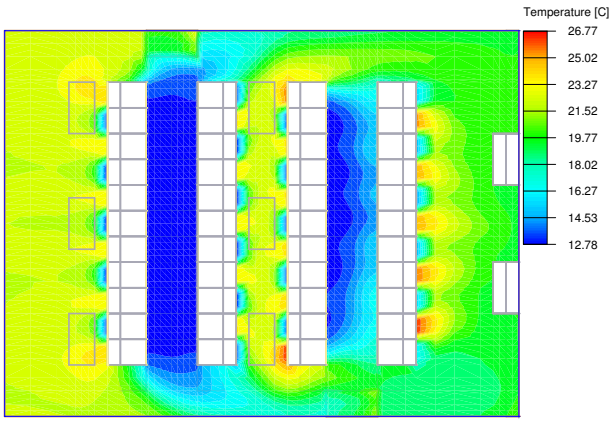

Figure 23: Temperature profile inside the data center for uniform workload distribution

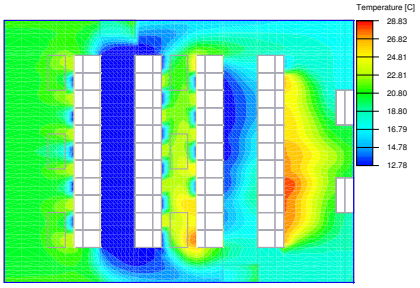

Figure 24: Temperature profile inside the data center after workload redistribution with heuristic-I for corner office

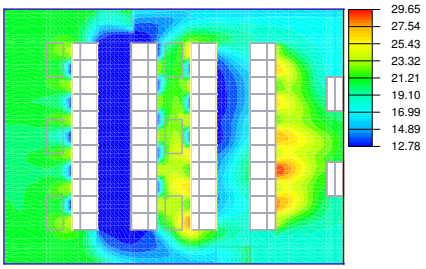

Figure 25: Temperature profile inside the data center after workload redistribution with heuristic-II for corner office

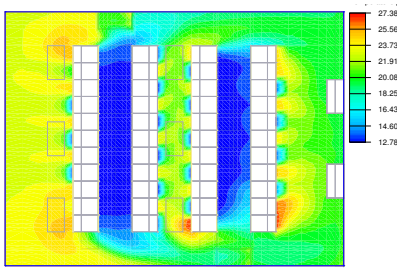

Figure 26: Temperature profile inside the data center after workload redistribution with heuristic-I for single mobile worker

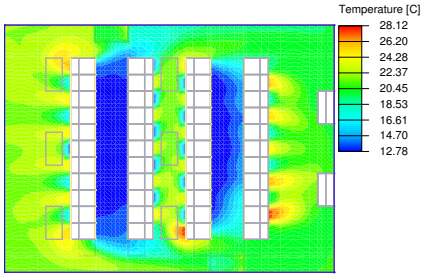

Figure 27: Temperature profile inside the data center after workload redistribution with heuristic-II for single mobile worker

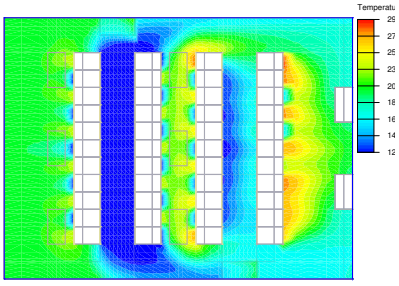

Figure 28: Temperature profile inside the data center after workload redistribution with heuristic-I for multiple workers

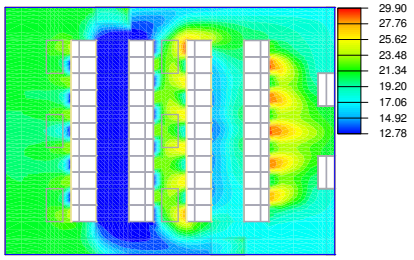

Figure 29: Temperature profile inside the data center after workload redistribution with heuristic-II for multiple workers

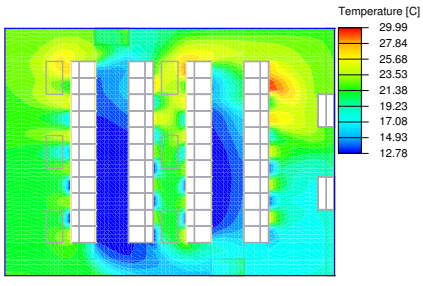

Figure 30: Temperature profile inside the data center after workload redistribution with heuristic-I for side wall

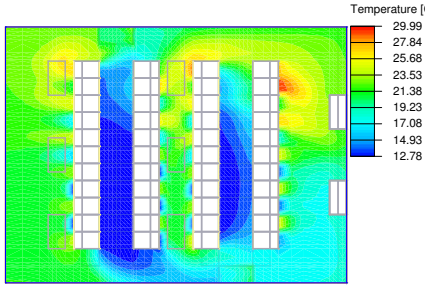

Figure 31: Temperature profile inside the data center after workload redistribution with heuristic-II for side wall

Combination of Parsec benchmarks run on a single server	Measured Power Consumption ($Watt$)
Idle	98.9
blackscholes	149.5
bodytrack	144.9
ferret	124.2
freqmine	126.5
swaptions	156.4
canneal	124.2
streamcluster	135.7
blackscholes bodytrack	170.2
blackscholes ferret	138
ferret streamcluster	151.8
freqmine swaptions	163.3
freqmine swaptions	190.9
freqmine swaptionsLarge	197.8
freqmine canneal	133.4
freqmine streamcluster	154.1
swaptions swaptions	197.8
blackscholes swaptions streamcluster	193.2
blackscholes swaptions canneal	197.8
bodytrack swaptions swaptions	202.4
bodytrack swaptions canneal	184.0
bodytrack swaptions streamcluster	190.9
ferret freqmine swaptions	172.5
blackscholes bodytrack freqmine streamcluster	190.9
blackscholes bodytrack swaptions canneal	197.8
blackscholes bodytrack swaptions streamcluster	195.5
bodytrack ferret swaptions canneal	190.9
bodytrack ferret swaptions streamcluster	195.5
freqmine swaptionsLarge canneal streamcluster	207.0
blackscholes ferret freqmine swaptions streamcluster	200.1
blackscholes bodytrack ferret freqmine swaptions streamcluster	202.4
blackscholes bodytrack ferret freqmine canneal streamcluster	202.4
blackscholes bodytrack ferret swaptions canneal streamcluster	195.5
blackscholes bodytrack freqmine swaptions canneal streamcluster	204.7
blackscholes ferret freqmine swaptions canneal streamcluster	200.1

Table 1: Parsec benchmarks with their measured power consumption